Journal of South American Earth Sciences 29 (2010) 817–831

Contents lists available at ScienceDirect

Journal of South American Earth Sciences

journal homepage: www.elsevier.com/locate/jsames

Paleomagnetic data and K–Ar ages from Mesozoic units of the Santa Marta massif: A preliminary interpretation for block rotation and translations

Germán Bayona [a,b,*], Giovanny Jiménez [a], César Silva [a,b], Agustín Cardona [a,b], Camilo Montes [a,b], Jairo Roncancio [c], Umberto Cordani [d]

[a] Corporación Geológica ARES, Calle 57 No. 24-11 of 202, Bogotá, Colombia
[b] Smithsonian Tropical Research Institute, Ancon, Panama
[c] Geosearch Ltda, Bogotá, Colombia
[d] Department of Geosciences, University of São Paulo, São Paulo, Brazil

ARTICLE INFO

Article history:
Received 23 December 2008
Accepted 26 October 2009

Keywords:
Santa Marta massif
Vertical-axis rotation
Terrane translation
Caribbean tectonics
Jurassic paleogeography

ABSTRACT

We report 6 K–Ar ages and paleomagnetic data from 28 sites collected in Jurassic, Lower Cretaceous and Paleocene rocks of the Santa Marta massif, to test previous hypothesis of rotations and translations of this massif, whose rock assemblage differs from other basement-cored ranges adjacent to the Guyana margin. Three magnetic components were identified in this study. A first component has a direction parallel to the present magnetic field and was uncovered in all units ($D = 352$, $I = 25.6$, $k = 57.35$, $a95 = 5.3$, $N = 12$). A second component was isolated in Cretaceous limestone and Jurassic volcaniclastic rocks ($D = 8.8$, $I = 8.3$, $k = 24.71$, $a95 = 13.7$, $N = 6$), and it was interpreted as of Early Cretaceous age. In Jurassic sites with this component, Early Cretaceous K–Ar ages obtained from this and previous studies are interpreted as reset ages. The third component was uncovered in eight sites of Jurassic volcaniclastic rocks, and its direction indicates negative shallow to moderate inclinations and northeastward declinations. K–Ar ages in these sites are of Early (196.5 ± 4.9 Ma) to early Late Jurassic age (156.6 ± 8.9 Ma). Due to local structural complexity and too few Cretaceous outcrops to perform a reliable unconformity test, we only used two sites with (1) K–Ar ages, (2) less structural complexity, and (3) reliable structural data for Jurassic and Cretaceous rocks. The mean direction of the Jurassic component is ($D = 20.4$, $I = -18.2$, $k = 46.9$, $a95 = 5.1$, $n = 18$ specimens from two sites). These paleomagnetic data support previous models of northward along-margin translations of Grenvillian-cored massifs. Additionally, clockwise vertical-axis rotation of this massif, with respect to the stable craton, is also documented; the sense of rotation is similar to that proposed for the Perija Range and other ranges of the southern Caribbean margin. More data is needed to confirm the magnitudes of rotations and translations.

1. Introduction

The allochthonous origin of continental basement blocks exposed between the Borde Llanero and Romeral fault systems in the northwestern corner of South America is a subject of debate (Fig. 1A). The Borde Llanero fault system separates poorly deformed Cretaceous and Cenozoic rocks of the Llanos basin (e.g., Cooper et al., 1995; Bayona et al., 2007) overlying deformed lower Paleozoic sedimentary rocks and Precambrian basement (Dueñas, 2002) with affinity to rocks exposed in the Guyana (Amazonian) craton (Priem et al., 1982; Ostos et al., 2005). The Romeral fault system bounds continental basement blocks to the east from oceanic-cored accreted terranes to the west (Estrada, 1995; Cediel et al., 2003; Kerr and Tarney, 2005). The Santa Marta massif is the northernmost continental basement block cored with Grenvillian-age metamorphic rocks; other blocks with similar basement rocks are the Bucaramanga-Floresta (Ward et al., 1973; Restrepo-Pace et al., 1997) and Garzon massifs (Cordani et al., 2005; Jiménez et al., 2006). When and how these terranes formed, collided and arrived to its present geographic position remains unclear. This paper reports new paleomagnetic and geochronological data from volcaniclastic and sedimentary rocks cropping out along the southeastern margin of the Santa Marta massif, that together with other paleomagnetic data presented in other tectonic blocks farther south, allow propose a model of how the Santa Marta massif arrived to its present position, and how the translations of terranes modified the present configuration of the northwestern corner of South America.

Detailed geochronological and geochemical analyses in granulite-cored basement uplifts of Grenvillian-age in the northern

* Corresponding author. Address: Corporación Geológica ARES, Calle 57 No. 24-11 of 202 Bogotá, Colombia. Tel./fax: +57 1 3101736.
E-mail address: gbayona@cgares.org (G. Bayona).

0895-9811/$ - see front matter © 2009 Elsevier Ltd. All rights reserved.
doi:10.1016/j.jsames.2009.10.005

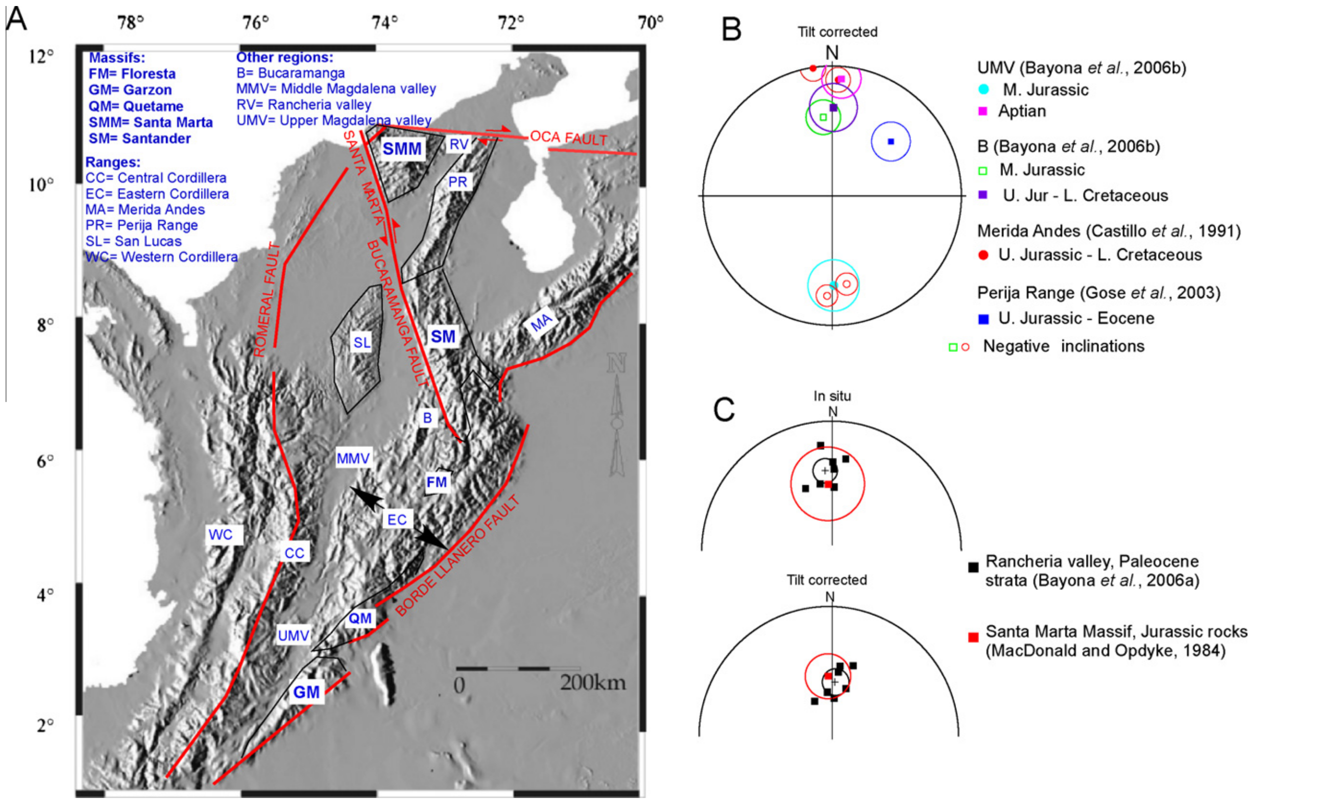

Fig. 1. (A) Location of massifs with grenvillian basement (SMM, SL, SM, GM) in the northern Andes; the Santa Marta massif is at the northernmost latitude. (B and C) Paleomagnetic directions reported in previous studies. Paleomagnetic direction in the Perija Range indicates clockwise rotations 50 ± 12° (Gose et al., 2003).

Andes reveal an affinity with terranes of Mexico and the Central Andes (Restrepo-Pace et al., 1997; Cordani et al., 2005). Fragmentation of these terranes took place during the early Paleozoic (Cordani et al., 2005), but collisions between Grenvillian-age basement blocks and Gondwana during the aggregation of Pangea remains uncertain (Silurian–Early Devonian, Forero, 1990; Restrepo-Pace, 1992). Recently, Cardona et al. (2010) based on a review geochronological data from Grenvillian basement and detrital signatures on younger Paleozoic orogens of Colombia, Ecuador and Peru, proposed that Grenville-cored massifs in Colombia, such as the Santa Marta massif were formed on the northwestern margin of the Amazonia craton, and subsequently become remobilized para-authochtonous during younger orogens.

Even though the age of igneous and metamorphic rocks are different among the Santa Marta massif, Perija range and the Merida Andes, paleomagnetic results from Middle Jurassic and younger rocks exposed in those ranges indicate no paleolatitudinal translations of allochthonous terranes since Middle Jurassic (Fig. 1B–D, Table 1). The core of the Santa Marta massif is grenvillian basement rocks (Restrepo-Pace et al., 1997; Cordani et al., 2005; Cardona-Molina et al., 2006), whereas the Merida Andes and Perija range are characterized by the absence of rocks older than 700 Ma (González de Juana et al., 1980; see more details for Merida Andes basement in PDVSA-INTEVEP, 2005). A thick cover of upper Paleozoic sedimentary rocks characterizes Perija and Merida ranges (Maze and Hargraves, 1984; Dasch, 1982; Forero, 1990), whereas upper Paleozoic sedimentary rocks are poorly recorded in the Santa Marta massif (Tschanz et al., 1974).

Bayona et al. (2006b) proposed along-margin northward translations of continental-cored terranes during the Early–Middle Jurassic on the basis of paleomagnetic data and integration of tectono-magmatic models for Late Triassic-Early Cretaceous time. Jurassic and Cretaceous units analyzed by Bayona et al. (2006b) include rocks exposed in the western block of the Bucaramanga fault (i.e. Bucaramanga area in Fig. 1), Floresta massif, and the southern Magdalena Valley (Fig. 1A and B). According to Bayona et al. (2006b), a linear, subduction-related, magmatic arc tectonic setting in the Late Triassic to Middle Jurassic (geochemical data summarized in Vásquez et al., 2006) was followed by the onset of intracontinental extensional and/or transtensional deformation with development of extensional basins since the Late Jurassic to the Early Cretaceous (as shown in Sarmiento-Rojas et al., 2006). However, several models considers that some of the Early to Middle Mesozoic geotectonic units west of the Guyana craton are in place, and constitute the westward growth of the plate margin (Mojica et al., 1996). The new paleomagnetic data presented in this study from Mesozoic rocks in the Santa Marta Massif, Colombian Caribbean, is used to refine the understanding and value of block translation hypothesis along the continental margin of northern South America.

2. Regional setting of the Santa Marta massif

The Santa Marta massif (SMM, Fig. 2A) comprises four lithotectonic belts (Tschanz et al., 1974) (Fig. 2). The northwestern corner consists of orthogneisses (92 Ma) and a low-grade metamorphosed volcanic-sedimentary belt (ca 82 Ma) with a Campanian age of metamorphism (MacDonald et al., 1971; Tschanz et al., 1974; Cardona et al., 2008). The second belt includes amphibolite facies rocks with a 530 Ma maximum protolith age and two-micas schist with associated Permian granitoids (Cardona-Molina et al., 2006; Cardona et al., 2008). The third belt consists of granulite facies and associated metamorphosed anorthosites with a 1.25 Ga protolith (Cordani et al., 2005) recording the Grenvillian continental col-

Table 1
Location, ages, directions and statistical parameters for Jurassic to Paleocene directions reported in previous studies (see Fig. 1).

Area	Unit	Site North°	Site West°	Age	N/s	In situ				Tilt-corrected				VGP			Paleolatitude		
						Dec.	Inc.	*k*	a95	Dec.	Inc.	*k*	a95	Latitude	Longitude	A95	Mean	Error-south	Error-north
Bucaramanga and Upper Magdalena Valley (Bayona et al., 2006a,b)																			
Bucaramanga	Jordán	7.25	73.15	L-M Jur.	2/13	15.1	−5.2	10.7	13.3	353.6	−27.1	15.0	11.1	67.5	123.2	8.9	−14.4	−21.5	−8.2
Bucaramanga	Girón	6.97	73.07	UJur.-LC	5	9.0	13.3	29.3	14.4	1.7	21.8	29.31	14.4	85.3	307.9	11.0	11.3	3.7	20.1
Floresta massif	Girón-Tibasosa	6.06	72.79	UJur.-LC	5	353.1	−14.8	12.8	22.2	352.6	14.8	33.0	13.5	82.5	208.9	9.9	7.5	0.7	15.1
Upper Magdalena	Saldaña	3.84	75.41	UTri.-LJu	7	175.2	15.2	16.0	14.3	178.9	20.3	14.5	75.21	75.6	109.0	11.4	−10.5	−19.6	−2.6
Upper Magdalena	Yaví3,4674,96Apti	3.46	74.96	Aptian	8	5.5	−5.4	74.96	10.4	5.2	6.2	40.2	9.6	85.7	5.4	6.8	3.1	1.7	8.1
Mérida Andes (Castillo et al., 1991)																			
Mérida Andes	La Quinta	8.1	71.8	M-U Jur.	1/18	172.8	−15.2	38.7	5.6	182.8	−17.4	36.2	5.8	87.1	1.7	4.31	8.9	5.9	12.1
Mérida Andes	La Quinta	8.1	71.8	M-U Jur.	1/14	352.1	16.1	39.1	6.4	351.6	0.1	51.7	5.6	78.4	154.6	3.96	0.1	−2.8	2.9
Mérida Andes	La Quinta	7.8	71.5	M-U Jur.	1/24	356.2	−49.7	35.6	6.5	3.1	5.9	41.9	6	84.3	76	4.24	3	−0.1	6
Mérida Andes	Rio Negro	7.8	71.5	L. Cr.	1/8	172.9	−7.9	74.4	6.5	170.4	−20.5	74.3	6.5	80.1	215.6	4.94	10.6	7.1	14.3
Santa Marta massif (MacDonald and Opdyke, 1984)																			
Bosconia	Guatapuri	10.1	73.7	UTri.-U.J	3	2.4	36.4		20.8	7.6	47.2		26.7	70.4	306.6	27.8	28.4	10.6	60
Valledupar	LosClavos	10.4	73.4	L-M Jur.	4	344.6	34.7		29.1	351.2	41.3		21.1	74.3	255	20.1	23.7	10.4	43.7
Perijá range Maze and Hargraves (1984)																			
Volcanic rocks	La Quinta	10.3	72.5	M-U Jur.	10	323	−2		28.4	319	9		35.9						
Red beds	La Quinta	10.3	72.5	M-U Jur.	5	311	0		36.1	309	3		35.7						
Dikes	La Quinta	10.3	725	M-U Jur.	3	354	36		10.4	6	27		16						
Gose et al. (2003)																			
|Perijá range	Several units	10.50	72.70	Jur-Eoc.	11					47.4	26.1	426	12.4	44.1	6.6	9.6			
Rancheria basin (Bayona et al., 2006a)																			
Cerrejone min	Hato Nuevo-Manantia	11.00	72.80	U Kr-Pale	8	357.7	26.9	41.3	8.7	8.6	45.6	34.3	9.6						

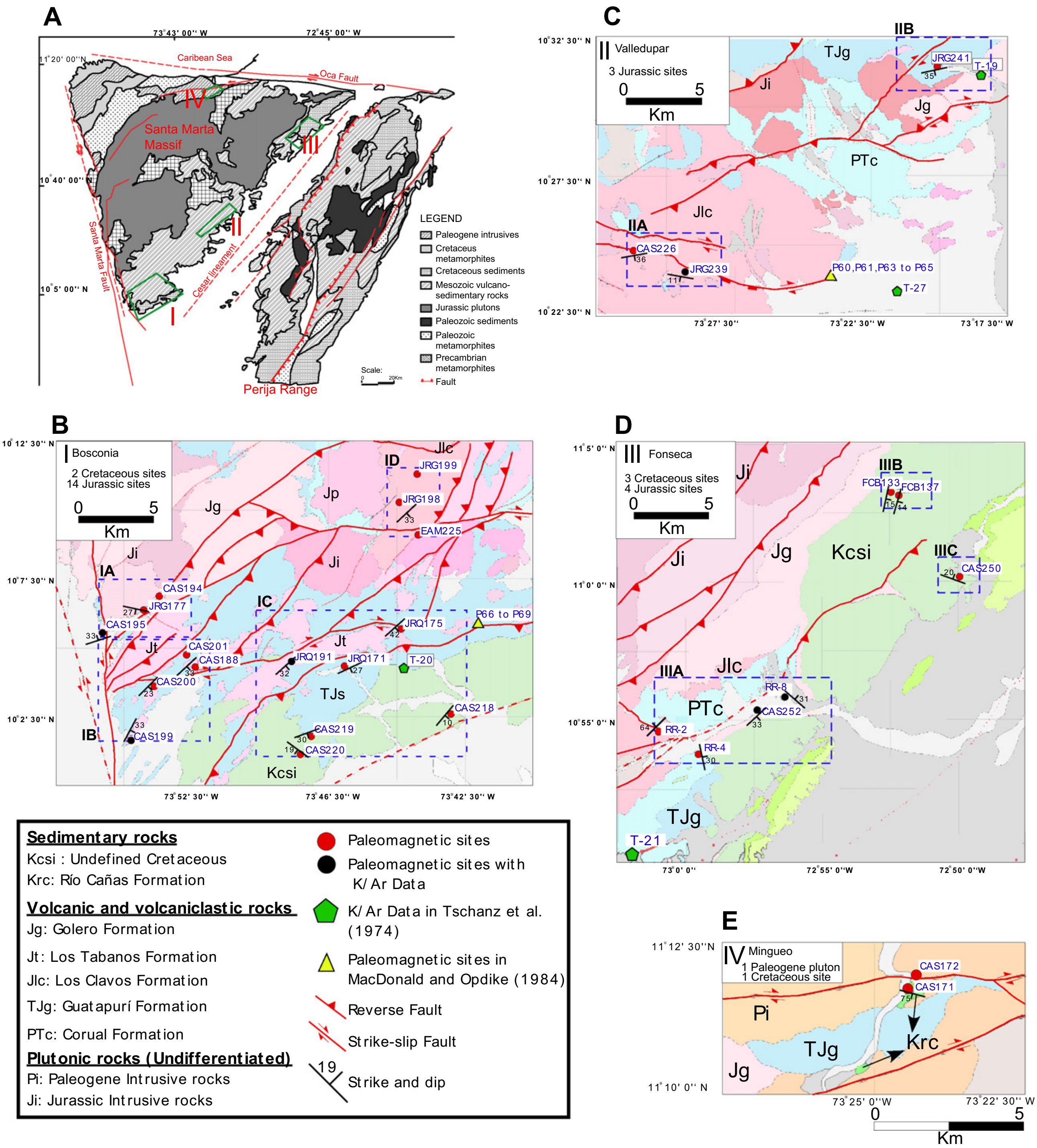

Fig. 2. (A) Simplified geologic map of the Santa Marta massif and Perija Range (modified from Bellizzia et al. (1976) and Tschanz et al. (1974)) showing the distribution of sites in four sectors, named I, II, III and IV. (B–E) Geologic map for each sector indicating the location of paleomagnetic sites (this study and MacDonald and Opdyke (1984)), stratigraphic units, major structures, and units with K–Ar ages (this study and Tschanz et al. (1974)).

lision at ca 1.16–0.9 Ga (Restrepo-Pace et al., 1997; Cordani et al., 2005). Isolated upper Paleozoic sedimentary rocks are also reported in this belt (Tschanz et al., 1969). Granitoids of Paleocene and Lower Eocene age intrude rocks of these three belts toward the northwest (Tschanz et al., 1969; Cardona et al., 2008), whereas granitoids of Jurassic age intrude the third belt and constitute the unit with greater surface area in the SMM. Along the southeastern border of Jurassic granitoids and volcanic units, Tschanz et al. (1974) documented Early Cretaceous and Paleocene reset of Jurassic granitoids. A fourth belt to the southeast consists of weakly deformed Triassic–Jurassic volcaniclastic and plutonic rocks unconformably overlain by Cretaceous–Paleocene sedimentary rocks. Paleomagnetic sites are located in this belt. The Perija range, to the southeast of the fourth belt and the Rancheria Valley, consist mainly of Jurassic volcaniclastic rocks (Maze and Hargraves, 1984) overlying upper Paleozoic sedimentary rocks and Lower Cretaceous rocks sedimentary accumulated in an extensional basin (Miller, 1962; Caceres et al., 1980).

Lithotectonics units described above are bounded by two major strike–slip faults (Fig. 2). The right-lateral Oca Fault to the north and the left-lateral Santa Marta Fault to the west places rocks of the four belts in contact with thick Neogene successions of the Guajira and Lower Magdalena basins, respectively. The Cretaceous–Paleocene sedimentary succession exposed in the fourth belt forms a low-angle, southeast-dipping homocline in structural continuity with rocks of the fourth belt of the SMM (Montes et al., 2005). Faults and folds disrupt locally the fourth belt that is bounded to the southeast by the Cesar lineament (Fig. 2A).

3. Study areas and sampling strategy

A total of 28 sites (307 specimens) were collected in Middle Jurassic volcanic and volcaniclastic rocks, Aptian–Albian calcareous units, and in a Paleocene pluton. Sites were distributed in four sectors, internally divided into structural domains to perform the tilt and unconformity test. Fig. 2 illustrates the structural domains in each sector, and below is a brief description of the sampled units (see Table 2 for more details). This work uses the stratigraphic nomenclature presented in the geologic map of Invemar–Ingeominas–Ecopetrol – ICP-Geosearch Ltda (2007).

The Bosconia sector (I in Fig. 2B), at the southwestern corner of the massif, includes four structural domains. Jurassic volcaniclastic rocks were sampled in domains IA and IB, which are located near the trace of the Santa Marta fault system. Domain IC follows the regional trend of Cretaceous calcareous beds (two sites) that unconformably overlie volcaniclastic rocks of the Guatapuri Formation (four sites). Three sites in domain ID were sampled in massive tuffs of the Los Clavos Formation, being these sites the most distant to the Santa Marta fault. Pre-Cretaceous rocks are affected by two reverse fault systems; the more regional with inferred right-lateral displacements. Additional mapping is needed to define whether strike-slip deformation took place along these two families, and the geometric–kinematic relationship with the left-lateral Santa Marta – Bucaramanga fault system.

Volcaniclastic rocks of Los Clavos and Guatapuri Formations crop out in the Valledupar sector (II in Fig. 2C), located to the northeast of sector I. Sites were located in two areas, the western domain (IIA, 2 sites) and the eastern domain (IIB, 1 site). In both areas, a dominant east-northeast-striking reverse to right-lateral fault system affects the Jurassic units. Other local faults without a uniform strike and displacement (reverse, normal and strike–slip) are present between the regional faults. As in the Bosconia area, a detailed structural analysis is needed to define the geometric–kinematic relationship between these two major fault systems.

The Fonseca sector (III in Fig. 2D), located at the northeastern corner of the massif, is bounded to the north by the Oca Fault system. In domain IIIA, four sites were drilled in Jurassic volcanic rocks of the Golero, Los Clavos and Guatapuri formations. Cretaceous calcareous beds unconformably overlie Jurassic beds, and three sites in Cretaceous rocks were collected in domains IIIB and IIIC. Even though northeast-trending faults, both strike–slip and northwest-verging reverse faults, have been mapped in this sector, its structural complexity is minor compared to the localities in Bosconia and Valledupar.

The Mingueo sector (IV in Fig. 2E) is located along the northern face of the massif and south of the Oca fault system. One site was collected in highly-deformed Lower Cretaceous calcareous and siliciclastic beds of the Rio Cañas Formation and another site in a Paleogene plutonic rock. East-striking, right-lateral fault systems parallel to Oca Fault. define blocks that include Paleogene intrusive rocks, Jurassic volcaniclastic strata and isolated outcrops of Lower Cretaceous rocks.

Samples from six sites of pre-Cretaceous volcanic rocks were selected to carry out whole-rock K–Ar crystallization ages, assuming no exotic Ar enrichment (Faure, 1986; Mcdougall and Harrison, 1999).

4. Paleomagnetic methods

Paleomagnetic samples were taken during the 2006–2007 field seasons of the Invemar–Ingeominas–Ecopetrol – ICP mapping project using a portable drill core and oriented with a magnetic compass. Two oriented hand samples were collected in site RR4 because they were located at the end of a tunnel under construction for the (Rancheria dam).

Alternate fields (AF) and thermal progressive demagnetization analysis were carried out at the Paleomagnetic laboratories of Sao Paulo University (AF) and the University of Florida (AF and thermal). Components of magnetization were calculated by means of Principal Component Analysis (Kirschvink, 1980) interpreted with the aid of orthogonal demagnetization diagrams (Zijderveld, 1967). Mean magnetization directions were calculated using Fisher's statistics (Fisher, 1953). Components with k values less than 10 are indicated as directions with high dispersion, and sites with k values less than 15 were not used for calculation of mean directions (Table 2).

Characteristic directions of Middle Jurassic units have two steps of tilt correction. Actual bedding (DD/D = dip direction/dip angle) indicate attitude of Middle Jurassic beds at present stage of deformation. For correction 1, we used the attitude of overlying Cretaceous beds to calculate mean-site directions and Cretaceous bedding for Jurassic beds (KrDD/KrD). Correction 2 calculates mean-site directions assuming that Jurassic beds accumulated on a horizontal surface.

Local incremental tilt tests (McFadden and Reid, 1982) were used to determine the timing of magnetization with respect to Cretaceous deformation. The significance of the tilt test followed the criteria of McElhinny (1964) because of the limited number of sites per structural domain. The mean VGPs (virtual geomagnetic poles) and paleolatitudes were determined from the characteristic components. Middle Jurassic to Early Cretaceous paleomagnatic poles for the South American cratonic areas (data from Castillo et al., 1991; Randall, 1998; Vizán et al., 2004) were used to determine the paleolatitude of a reference point in the Colombian craton and to estimate the difference of northward displacement among the Santa Marta massif, other grenville-cored massifs in Colombia, and the reference point in the Colombian craton. For vertical-axis rotations, the confidence limits for structural domain declinations and the relative difference of declinations with an arbitrary point in the stable craton follow the criteria given by Demarest (1983).

5. Paleomagnetic results

Demagnetization diagrams for the studied Mesozoic strata show univectorial and multivectorial paths, the latter suggesting at least two events of magnetization. Directions of magnetization were grouped in five components according to: (1) their temperature/coercivity range (see Table 2 for details) and (2) the behaviour of their directions before and after tilt corrections. Components A and B precede characteristic components C1, C2 and C3.

Components A and B were uncovered dominantly at low to moderate temperature/coercivity ranges, and for component A normal and reverse directions were determined. Component A was isolated in 14 sites distributed in the four sectors, including the Paleogene intrusive rocks (Fig. 3A), but only 12 sites have $k > 15$. The directions before tilt correction have a northward

Table 2
Statistical parameters of mean-site directions uncovered in 28 sites analyzed in the Santa Marta massif. DD/D = dip direction/dip angle; KrDD/KrD = corrected Cretaceous bedding for Jurassic beds; N/n = total specimens/specimens used for mean calculation; D = Declination; I = Inclination, *k* = the Fisher (1953) precision parameter; a95 = half-angle of 95% confidence about the mean for sites. See text for discussion about tilt corrections.

Sector	Area	Site	Unit	Rock Description	Actual DD/D	Overlying Cretaceous DD/D	KrDD/KrD	N/n	range	In situ				Correction 1		Correction 2		Component
										Dec	Inc	*k*	a95	Dec	Inc	Dec	Inc	
(I) BOSCONIA	IA	JRG177	Golero Fm.	felsic vitric tuff	192/27	130/10	188/22*	9/7	0-10 mT; 0-200 ºC	356,5	21,2	27,52	11,7	359,9	27,9	356,8	49,6	A
								9/9	10-100 mT; 200-620 ºC	358,2	17,5	3,74	30,9	High Dispersion to the North				
		CAS194	Golero Fm.	felsic vitric tuff	192/27 &	130/10	188/22*	8/8	0-20 mT; 0-300 ºC	352,2	23,7	96,06	5,7	355,8	30,9	350,8	52,2	A
								7/7	20-90 mT; 300-680 ºC	188,2	23,9	22,91	12,9	185	18,4	185,1	-3,5	C2(reverse)
		CAS195	Golero Fm.	latitic tuff (p)	342/33	110/21	356/44	4/3	0-30 mT	354	25,4	37,39	20,5	5,1	32,8	3,8	-10,7	A
	IB	CAS188	Tábanos Fm.	latitic crystal vitric tuff (p)	137/33 &	130/10	136/23 *	6/6	10-100 mT; 0-200 ºC	348,9	28,7	32,87	11,9	353	36,3	9,4	52,7	A
								6/5	200-620 ºC	61,8	12,5	103,6	7,6	63,5	8,6	65,4	1,2	C3
		CAS199	Guatapurí Fm.	latitic vitric tuff (p)	118/33	130/10	119/23*	7/6	0-200 ºC	345,1	32,1	44,28	10,2	349,6	40,1	10,7	51,5	A
								7/7	400-620 ºC	352	2	27,33	11,8	352,7	9,3	358,2	22,2	C1
		CAS200	Guatapurí Fm.	tuffaceous siltstone	135/23	130/10	134/13*	4/8	0-50 mT; 100-300 ºC	327	12,8	14,36	25,1	328	22,3	329,8	34,9	A**
								8/8	50-100 mT; 400-660 ºC	359,8	2,5	38,2	9,1	0,6	9	2,9	17,7	C1
		CAS201	Tábanos Fm.	felsic vitric tuff	137/33 &	130/10	136/23 *	6/5	0-100 mT; 0-500 ºC	340,8	24,1	28,78	14,5	343,7	32,6	355,5	51,9	A
	IC	JRQ175	Guatapurí Fm.	tuffaceous siltstone and lithic tuff	138/42	130/10	137/32 *	5/5	0-300 ºC	0,3	4,3	89,93	8,1	1,3	10,6	11	31,9	A
								5/4	300-660 ºC	14,3	1,5	232,8	6	14,9	5,8	21,8	21,4	C1
		JRQ171	Guatapurí Fm.		155/27	130/10	153/18*	6/4	0-450 ºC	30,7	5,4	28,19	17,6	31,8	6,9	35	15,9	C1
		CAS219	Guatapurí Fm.	lithic-crystal felsic lapilli tuff	160/30	216/19	167/18	10/8	0-25 mT; 0-300 ºC	343,5	21,2	22,08	12,1	335,5	31,8	332	49,3	A
								10/7	0-100 mT; 300-640 ºC	High Dispersion								
		JRG191	Guatapurí Fm.	latitic tuff (p)	138/32	130/10	137/22*	6/6	0-400 ºC	High Dispersion								
								6/6	400-700 ºC	16,9	-11,9	208,6	4,6	15,3	-7,9	14,6	3,9	C2
		CAS218	Undifferentiated Cretaceous	biomicrite, wackstone	130/10			6/2	0-560 ºC	High Dispersion								
								6/4	0-700 ºC	200,3	-1,9	126,13	8,2	200,9	-5,2			C1(reverse)
		CAS220	Undifferentiated Cretaceous	micrite	216/19			5/4	0-300 ºC	High Dispersion								
								5/5	300-450 ºC	352,7	-2,1	34,96	13,1	351,5	11,7			C1
	ID	JRG198	Los Clavos Fm.	quartztrachytic vitric-cystal tuff (p)	137/33 &	130/10	136/23 *	7/6	0-15 mT; 0-400 ºC	High Dispersion								
								7/6	15-100 mT; 400-590 ºC	29,7	-15,6	61,78	9,8	27,2	-13,5	23,5	-5,3	C2
		JRG199	Los Clavos Fm	latitic crystal-lithic tuff	137/33 &	130/10	136/23 *	6/4	0-15 mT; 100-400 ºC	High Dispersion								
								6/5	30-100 mT; 530-620 ºC	358,8	-27,9	14,66	20,7	355,4	-21,1	352,4	-2,9	C2**
		EAM225	Los Clavos Fm	intermediate tuff	137/33 &	130/10	136/23 *	6/6	0-15 mT;y 0-300 ºC	High Dispersion								
								6/5	15-100 mT; 450-620 ºC	24,8	-35,7	61,16	9,9	18,3	-32,5	8,6	-20	C2
(II) VALLEDUPAR	IIA	JRG239	Los Clavos Fm	trachytic lithic-crystal tuff (p)	190/11	130/10	189/6*	8/6	0-12.5 mT; 0-300 ºC	High Dispersion								
								8/8	12.5-100 mT; 300-590 ºC	4,1	-38	9,94	18,5	358,6	-31,7	359,2	-25	C2**
		CAS226	Los Clavos Fm	latitic crystal-vitric tuff	170/36	130/10	166/28*	6/4	0-100 mT; 0-300 ºC	High Dispersion								
								6/5	0-100 mT; 500-590 ºC	340,4	-45,9	37,09	12,7	336,2	-37,1	338,1	-9,4	C2
	IIB	JRG241	Guatapurí Fm.	tuffaceous siltstone	168/35	130/10	164/27*	7/1	0-450 ºC	High Dispersion								
								7/6	0-660 ºC	2,1	-7,9	10,72	21,4	1,4	-1,7	3,1	24	C1**
(III) FONSECA	IIIA	CAS252	Golero Fm.	dacitic tuff (p)	137/33 &	140/10.5	137/22*	8/7	0-7 mT; 100-400 ºC	188,8	-27,4	14,92	16,2	193,7	-33,9	209,9	-43,5	A**(reverse)
								8/8	10-origen; 500-590 ºC	29,7	58,1	35	9,5	47,1	60,3	80,3	53,6	C3
		RR2	Los Clavos Fm	crystal-vitric tuff	315/64 +	140/10.5	311/74*	14/12	0-15 mT; 0-300 ºC	High Dispersion								
								14/14	25-100 mT; 500-590 ºC	32,9	-18	15,26	10,5	29,9	-14,7	52,4	-14,4	C2
		RR4	Guatapurí Fm.	tuffaceous siltstone	78/30	140/10.5	83/25*	13/12	0-10 mT; 0-300 ºC	High Dispersion								
								13/13	35-100 mT; 500-680 ºC	30,8	-7,7	125,27	3,7	29,8	-4,1	25,6	-18,5	C2
		RR8	Los Clavos Fm	andesitic to latitic tuff (p)	41/31	140/10.5	47/32*	8/4	0-50 mT; 0-500 ºC	323	0,1	33,98	16	323	10,6	327,7	5,8	B
								8/5	25-100 mT; 100-660 ºC	7,7	1,2	43,94	11,7	8,3	8,2	6,8	-16,8	C2
	IIIB	FCB133	Undifferentiated Cretaceous	biomicrite, wackstone	102/15			6/5	90-origen; 0-590 ºC	357,7	31,8	131,46	6,7	7,4	34,3			A
		FCB137	Undifferentiated Cretaceous	biomicrite, packstone	106/14			6/6	90-origen; 0-400 ºC	350,9	28,8	103,7	6,6	358,9	33,8			A
	IIIC	CAS250	Rio Cañas Formation	micrite	20/20			6/4	0-200 ºC	346	33,2	47,53	13,5	350,8	16,1			A
								6/4	200-500 ºC	218,8	-7	27,08	18	219,1	11,9			B
(IV) MINGUEO		CAS172	Santa Marta Batholith	quartz-monzonite				6/4	0-300 ºC	349,8	11,1	12,05	18,1					A**
								6/4	300-560 ºC	190	-29,2	20,83	20,6					A(reverse)
		CAS171	Rio Cañas Fm.	biomicrite and calcareous siltstone	195/75			6/5	0-20 mT	High Dispersion								
								6/5	7.5-50 mT	1	-39,9	28,18	14,7	2,1	33,6			C1**

(p) sample with petrography
& for sites without signals of stratification in volcanic rocks, we consider the regional attitude from adjacent sites of the same sector
+ High deformation in site RR2. DD/D data is an approximation, but it is not reliable
* where Cretaceous rocks are not exposed, we use the regional attitude of Cretaceous units for tilt correction (DD/D= 130/10)
** sites with k<15 were not used for calculation of mean directions of sectors shown in Table 3 and in Figure 4

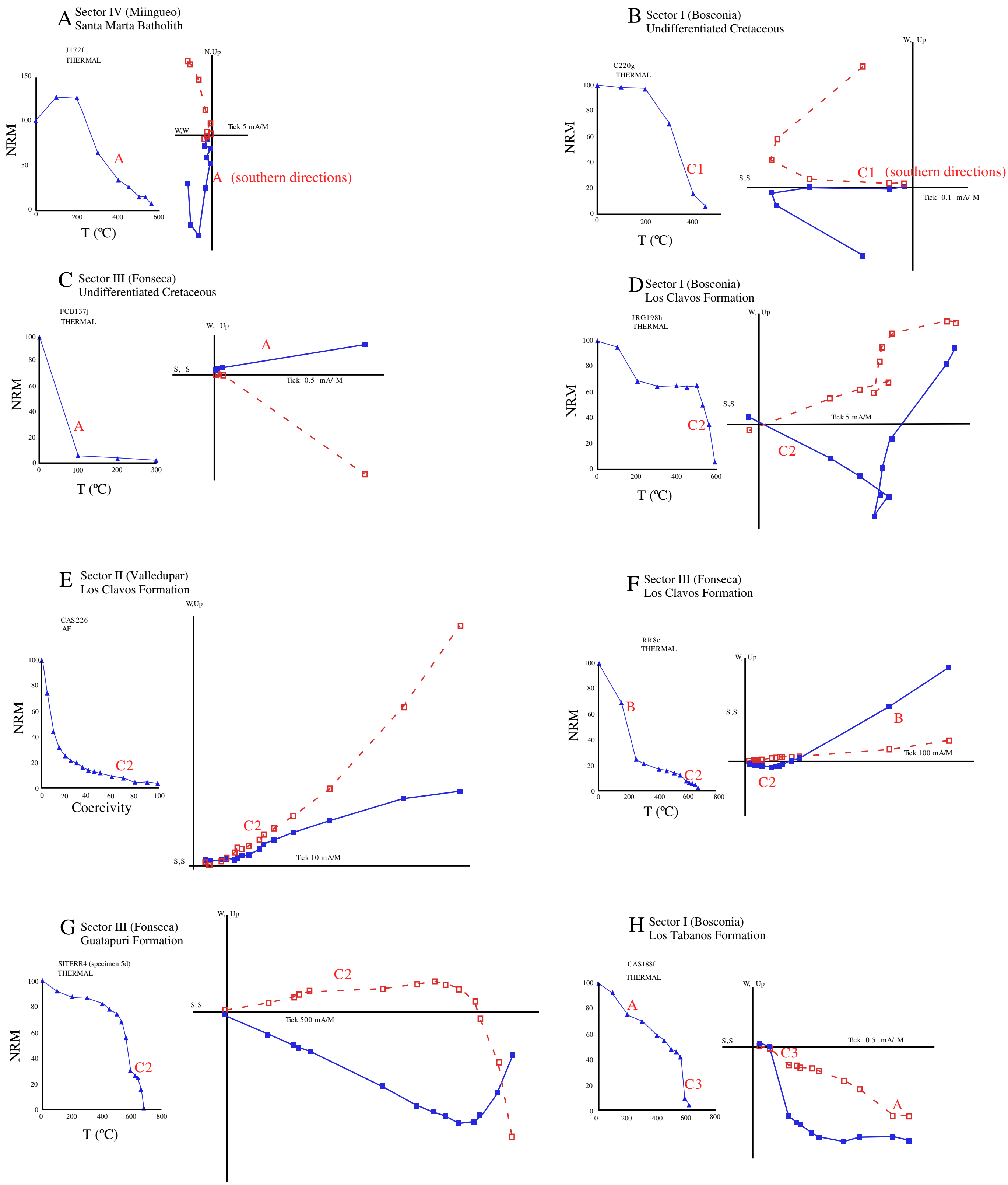

Fig. 3. Orthogonal diagrams of demagnetization of representative samples before tilt correction. Full (open) symbols in Zijderveld plots represent projections onto the horizontal (vertical) plane.

declination and shallow positive inclination (Fig. 3C and H) or the equivalent reverse (Fig. 3A). Directions of component A show the best grouping before tilt correction using 12 sites (Fig. 4, Table 4). Directions and unblocking temperatures/coercitivity of component B are not uniform, although they were uncovered at less than 500 °C. In site RR8 (Jurassic unit) Component B precede a characteristic component C2 and in site CAS250 (Cretaceous unit) is at higher ranges of Component A.

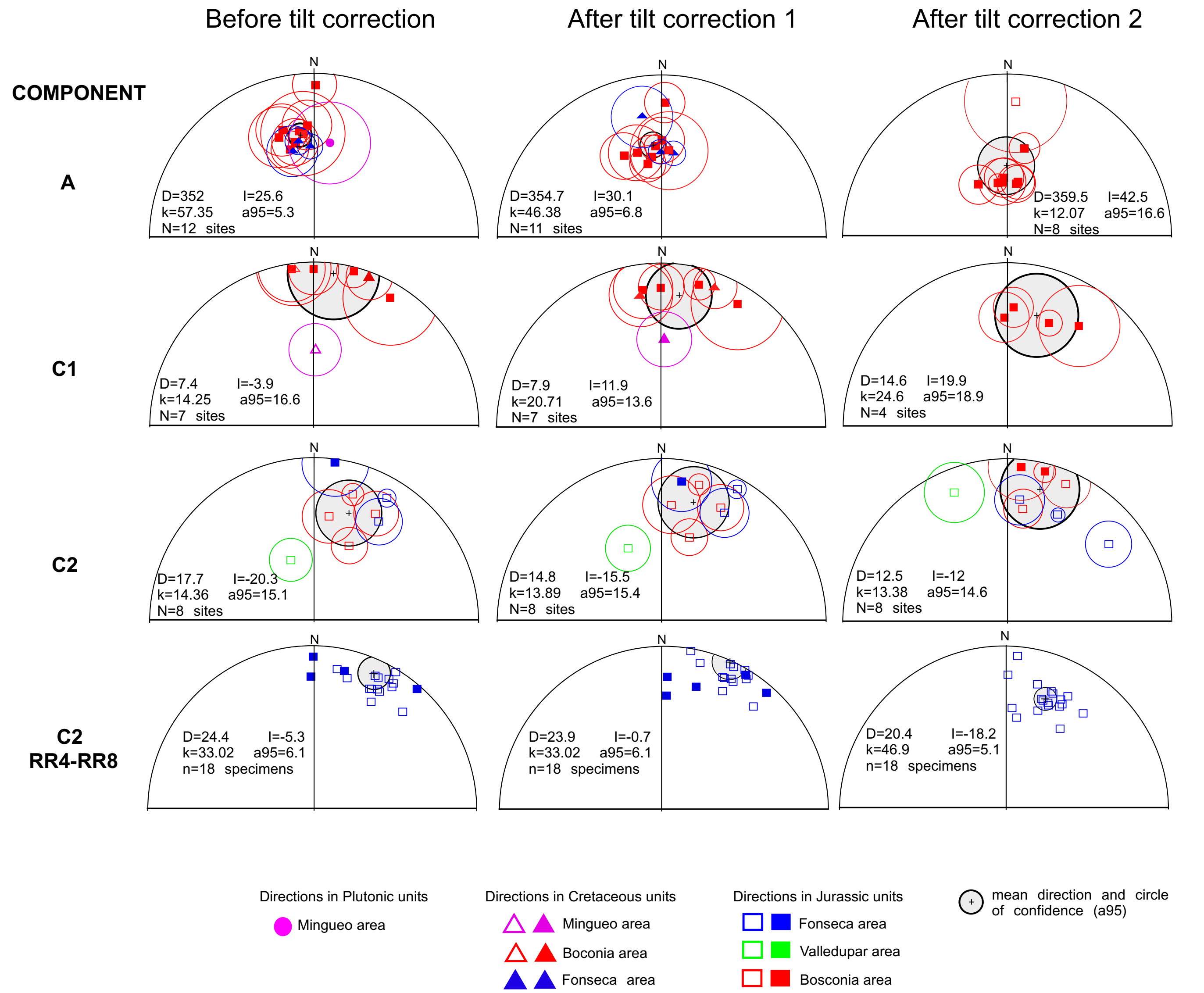

Fig. 4. Equal-area plots at different ages and sectors showing tilt-corrected directions of paleomagnetic components A, C1 and C2. Solid (open) symbols represent positive (negative) inclinations.

A characteristic component C1, uncovered at moderate to high-temperature/coercivity ranges (Table 2), was isolated in Cretaceous and Jurassic rocks from Bosconia (six sites, Fig. 3B), Valledupar (1 site with $k < 15$) and Mingueo (1 site with $k < 15$). In situ directions of component C1 are north–northeastward with very shallow directions in sector I (Bosconia, or the equivalent reverse in site CAS218), and with moderate negative inclinations in sectors II (Valledupar) and IV (Mingueo). After tilt correction for Cretaceous bedding, directions of sectors I and IV have positive inclinations, whereas direction of sector II is almost flat (Fig. 4, Table 3), increasing the grouping coefficient k of the mean direction.

A characteristic component C2, uncovered at high-temperature/coercivity ranges (Table 3), was isolated in 11 sites with Middle Jurassic rocks in sectors I (Bosconia, Fig. 3D), II (Valledupar, Fig. 3E) and III (Fonseca. Fig. 3F and G). Directions of component C2 before tilt correction is mainly to the north with negative inclinations (Fig. 4, Table 3) or the equivalent reverse (southern directions in sites RR4 and CAS194 were converted to northward direction for calculation of mean directions). After the two-step tilt corrections, inclinations become shallower but continue negative, with exception of two sites that are very shallow with positive inclinations (Fig. 4). Declination values vary from north–northeast for sectors I and III, and more to the northwest for sector II.

Component C3, uncovered at moderate to high-temperature/coercivity ranges (Table 2), was defined in two sites, in sectors I and III (Fig. 3H). After the two steps of tilt correction, declination values are to the northeast–east but with disperse values of positive inclination (Table 2).

6. K–Ar analysis

6.1. Methods

Whole rock fragments were analyzed by the K–Ar method at the Centre of Geochronological Research of the University of São Paulo (CPGeo-USP). Analytical procedures are described in Cordani (1970) and Cordani et al. (2004). Two aliquots from the same sample were separated for the K and Ar analysis. Potassium analyses of each pulverized sample were carried out in duplicate, by flame photometry. Argon extractions were made in an ultra-high-vacuum system, where a spike of 38 Ar was added and the gas was purified in titanium and copper getters. Final argon isotopic determinations were carried out in a Reynolds-type gas spectrometer. Analytical precision for K, based on the duplicate analyses, is usually below 4% whereas for Ar it is around 0.5%. Decay constant of ^{40}K is after Steiger and Jager (1977).

6.2. Results

Table 4 presents age distribution of sampled sites, including previous K–Ar data from Tschanz et al. (1974). Samples from three sites (CAS195, JRG239 and CAS 252) report ages overlapping within error, which suggest that results reflect the evolution of the K–Ar system in the sampled area.

K–Ar ages reported in the Bosconia sector range from Early Cretaceous in Golero and Guatapuri volcanic rocks (CAS195, ca. 130 Ma in two samples with overlapping ages; 138 ± 9 Ma reported by Tschanz et al. (1974)), to Early Jurassic (JRG191, 196.5 ± 4.9 Ma) and to Permian in Guatapuri Formation (CAS199, ca 286 Ma in one sample with overlapping ages).

In the Valledupar sector, reported ages for Los Clavos and Guatapuri Formation range from Early Cretaceous (JRG239 yield two similar ages of 123 Ma, 133 ± 5 Ma reported by Tschanz et al. (1974)) to Early–Middle Jurassic (ca 175–180 Ma) according to three ages reported by Tschanz et al. (1974). In the Fonseca area, K–Ar ages are Late Jurassic, as indicated by two samples with overlapping ages from dacitic tuffs of Golero Formation (CAS 252, ca 152 Ma) and an andesite tuff of Los Clavos Formation (RR8, 156.6 ± 8.9 Ma). Farther to the south, Tschanz et al. (1974) report two Middle Jurassic ages in the Guatapuri Formation (165 ± 6 and 181 ± 10 Ma). Early to Middle Jurassic K–Ar ages obtained in volcanic rocks are within the range of U–Pb zircons ages reported from Jurassic plutons cropping out to the northwest (Bosconia: 175–180 Ma; Fonseca: 181–187 Ma; Invemar–Ingeominas–Ecopetrol – ICP-Geosearch Ltda, 2007) and with K–Ar ages reported by Tschanz et al. (1974).

Table 3
Statistical parameters of mean-site directions uncovered for each component in each sector. Abbreviations as in Table 2.

Component/sector	Sites (N/n)	In situ				Correction 1				Correction 2			
		Dec	Inc	*k*	a95	Dec	Inc	*k*	a95	Dec	Inc	*k*	a95
Componet A													
(I) Bosconia	16/8	350.3	22.7	61.11	7.1	353.2	30.7	44.46	8.4	359.5	42.5	12.07	16.6
(III) Fonseca	7/3	351.6	31.4	219.36	8.3	358.6	28.3	40.76	19.6				
(IV) Mingueo	2/1	190	−29.2	20.83	20.6								
Mean of Component A	28/12	**352**	**25.6**	**57.35**	**5.3**	354.7	30.1	46.38	6.8	359.5	42.5	12.07	16.6
Component C1													
(I) Bosconia	16/6	8.2	1.9	25.68	13.5	**8.8**	**8.3**	**24.71**	13.7	14.6	19.9	24.6	18.9
(IV) Mingueo [a]	2/1	1	−39.9	28.18	14.7	2.1	33.6	28.18	14.7				
Mean of Component C1	7	7.4	−3.9	14.25	16.6	1.9	19.9	20.71	13.6	14.6	19.9	24.6	18.9
Component C2													
(I) Bosconia	16/4	19.8	−22	35.14	15.6	16.3	−18.2	35.2	15.8	13	−4.5	34.83	15.4
(II) Valledupar	3/1	340.4	−45.9	37.09	12.7	336.2	37.1	37.09	12.7	338.1	−9.4	37.09	12.7
(III) Fonseca	7/3	23.6	−8.3	23.41	26.1	22.6	−3.5	23.39	26.1	28.2	−17.3	13.62	34.8
Mean of Component C2	8	17.7	−20.2	14.36	15.1	14.8	−15.5	13.89	15.4	12.5	−12	13.38	14.6
Mean of Component C2 (Sites RR4 and RR8 in Fonseca) [b]	21/18 (specimen level)	24.4	−5.3	33.02	6.1	23.9	−0.7	33.02	6.1	**20.4**	**−18.2**	**46.9**	**5.1**

Mean direction of components A, C1 and C2 used for other analysis are indicated in bold.
[a] Site with high structural deformation; therefore, we use mean value of Bosconia for calculation of VGP and paleolatitudes in Table 5.
[b] Site RR2 in Fonseca was excluded due to lack of reliable structural data, as indicated in Table 2.

Table 4
Analytical results of K–Ar data from our study and other K–Ar ages reported in volcanic rocks by Tschanz et al. (1974).

Data from this study (whole rock analysis)							
Sector	Area	Sample	Unit	%K	Rad ^{40}Ar, ccSTP/g x	Atm ^{40}Ar%	Age, Ma[*]
I BOSCONIA	IA	CAS 195 a	Golero Fm.	1978	10.61	10.2	133.0 ± 3.2
		CAS 195 b	Golero Fm.	2995	15.45	7.8	128.2 ± 2.7
	IC	JRG191b	Guatapuri Fm.	3653	29.45	8.8	196.5 ± 4.9
	ID	CAS 199 d	Guatapuri Fm.	1775	21.03	3.5	281.8 ± 6.3
		CAS 199 d REP	Guatapuri Fm.	1775	21.98	8.6	293.5 ± 6.8
II VALLEDUPAR	IiA	JRG 239 a	Los Clavos Fm.	3047	14.74	13.2	120.5 ± 3.1
		JRG 239 g	Los Clavos Fm.	3209	16.36	5.1	126.7 ± 2.7
		CAS 252 a	Golero Fm.	1456	9.02	8.3	152.9 ± 4.0
		CAS 252 e	Golero Fm.	1457	8.93	9	**151.3** ± 3.9
III FONSECA	IIIA	RR8	Los Clavos Fm.	0904	5.74	45.6	156.6 ± 8.9

Ages reported in volcanic rocks (Tschanz et al. (1974); pgl = plagioclase; hn = hornblende; ep = epidote; bt = biotite; wh r = whole rock)				
Sector	Sample code	Unit	Rock classification	Age, Ma
1 BOSCONIA	T-20 (Near site JRQ171)	Guatapuri Fm.	Basalt, intrudes?	138 ± 9 (pgl)
II VALLEDUPAR	T-19(Near siteJRG241)	Los Clavos Fm.	Rhyodacite ignimbrite	133 ± 5(pgl); 175 ± 13(hn); 180 ± 12 (hn + ep)
	T-27(Near site JRG239)	Stock in Los Clavos Fm.	Granodiorite stock	176 ± 7 (bt)
III FONSECA	T-21 (further south of site RR8)	Guatapuri Fm.	Basalt, below red beds	165 ± 6 (wh r); 181 ± 10 (wh r)

7. Discussion

7.1. Age of pre-Cretaceous volcaniclastic rocks

One difficulty along the southeastern margin of the Santa Marta massif has been the recognition of volcanic units. Two groups of K–Ar ages can be differentiated using the data presented here and those published by Tschanz et al. (1974). The older group corresponds to Early Jurassic to early Late Jurassic magmatic event(s) (ca 151–196 Ma) and includes K–Ar ages reported in the Bosconia, Valledupar and Fonseca sectors. This event is further supported by the reported K–Ar ages (Tschanz et al., 1974) and and U/Pb zircon ages (Invemar–Ingeominas–Ecopetrol – ICP-Geosearch Ltda, unpublished data) in Jurassic batholiths to the northwest. These two peak events are widespread along the Eastern Colombian Jurassic magmatic rocks (Aspden et al., 1987).

The second group is of Early Cretaceous age (120–138 Ma). These ages have been only reported in Bosconia (sites near the Santa Marta fault system) and Valledupar areas. Some of the early Cretaceous ages are in the same volcanic unit with reported Jurassic ages (e.g., sample T-19 and T-27, Table 4); therefore, we infer that these Early Cretaceous ages are reset ages due to heating related to an extensional tectonism that affected the adjacent Perija range and areas to the south of the Santa Marta-Bucaramanga fault system during latest Jurassic and Early Cretaceous time (Miller, 1962; Tschanz et al., 1974; Bellizzia et al. 1976; Caceres et al., 1980; Clavijo et al., 2008).

The Permian ages from the Guatapurí Formation (CAS199) are related to excess Ar. More detailed geochronology, including Ar–Ar analyses in feldspars and U–Pb ages, will allow to test the thermal significance of this Early Cretaceous event, the excess Ar linked to the Guatapuri Formation, and the detail stratigraphy of all these volcanic units.

7.2. Timing of magnetization of uncovered components

Directions of component A, uncovered in Paleogene, Cretaceous and Jurassic rocks (Table 2), are interpreted as thermoviscous or chemical re-magnetizations whose directions are either parallel to the present Earth magnetic field or have high dispersion. Northward and moderate positive directions reported by MacDonald and Opdyke (1984) correspond to low coercivity components (Table 1), and their directions are similar to the directions grouped as component A in this work. Similar directions were reported for Paleocene rocks in the Rancheria Valley by Bayona et al. (2006a)(Table 1), and they were interpreted as post-tilting. Therefore, we consider that the age of magnetization is post-tilting of Paleocene–Lower Eocene strata of the Rancheria Valley, likely of Miocene age or younger.

Directions of component C1 with $k > 15$ were uncovered in Cretaceous and Jurassic rocks in 6 sites of Bosconia (where we interpreted the reset of K–Ar ages). Directions have the best grouping after tilt correction for Cretaceous bedding (Fig. 4, Table 3); the inclination is shallow and positive, but declinations have a large dispersion to the north–northeast. Although dominant southeast dip trend of strata exposed in Bosconia limit the options for reliable tilt tests, the drift from negative to positive inclination of the mean direction of a Cretaceous site in sector IV (Mingueo) support the idea of a pre-tilt magnetization age for C1 component (Fig. 4). Two additional arguments can be used to propose Early Cretaceous age of magnetization for Component C1. First, the reset ages, inferred from heating, are Early Cretaceous and affect some sites near the Santa Marta fault (sector I) but do not affect sites faraway (sector III). Secondly, directions determined for other Lower Cretaceous rocks in the Merida Andes (Castillo et al., 1991), Perija Range (Gose et al., 2003), Bucaramanga, Floresta and southern Magdalena Valley (Bayona et al., 2006b) have similar inclinations (Fig. 1, Table 1).

Directions of component C2, uncovered in Jurassic volcaniclastic rocks distant to the Santa Marta fault system, have inclinations values that differ from the inclinations of components A and C1. In sectors I, II and III the dominant negative inclinations persist after the two stages of tilt correction (or very shallow positive in some sites) (Fig. 4, Table 3), indicate that the direction of component C2 is different from overlying Cretaceous beds (positive unconformity test). Although C1 and C2 components were not uncovered in a single site of Jurassic rocks, these components were uncovered in adjacent areas where Jurassic and Cretaceous rocks were exposed (areas IC and ID, Table 2). A near depositional magnetization of characteristic direction C2 isolated in Jurassic rocks is inferred by: (1) Declinations/Inclination values are different in comparison with the present magnetic field or directions of Component A (uncovered in Paleogene rocks) and with characteristic directions uncovered in Cretaceous rocks (Component C1) after tilt correction (Fig. 4, Table 3); (2) high stability of components carried by minerals with unblocking temperature above 570 °C and 70 mT (e.g., titano-magnetite and hematite, Table 2); (3) better cluster of moderate negative inclinations after the two steps of tilt corrections; (4) sites with Component C2 has no reset ages (site JRG191 in area IC and site RR8 in area IIIA). Similar directions with negative inclinations were uncovered in the Middle Jurassic Jordan Formation in Bucaramanga area and Saldaña Formation in the southern Magdalena Valley (Fig. 1B, Table 1; Bayona et al., 2006b).

Directions of components B and C3 have not consistency, and we consider that they do not have a geological significance.

7.3. Vertical-axis rotations and translations: preliminary interpretations

After considering that the timing of magnetization of components C1 and C2 are Lower Cretaceous and Middle Jurassic in age, respectively, we can infer vertical-axis rotations and tectonic translations of the Santa Marta massif. Calculation of the declination/inclination values deducted for a stable point in the craton for Middle Jurassic time (see Bayona et al., 2006b for paleopoles of the South America craton) indicate that characteristic directions C1 and C2, whose declinations significantly differ from the North–South line, can be interpreted as belonging to blocks with some degree of vertical-axis rotation.

We need to consider local structural complexities that affect the directions of components C1 and C2 before using them for regional interpretations. The complex arrange of faults in sectors I and II, that include at least two families of faults affecting pre-Cretaceous units, may generate local rotations that increase the dispersion of declination values in these two sectors. In addition, we had to infer bedding attitude for some Jurassic sites (e.g., sites in area ID), as well as to consider a regional bedding attitude for Cretaceous beds where they are not exposed (e.g., sector II). For those reasons, even though the Middle Jurassic component C2 was uncovered in a total of 8 sites with k values >15 (Table 3), we used only sites RR4 and RR8 to calculate the mean direction (at specimen level, Table 3) of Component C2 for Fonseca sector (III) because: (1) sector III (Fonseca) is not affected by the Oca and Santa Marta fault systems and has the least internal complexity of all sites analyzed; (2) sites RR4 and RR8 have reliable structural data, whereas site RR2 does not have reliable attitude data and is affected by two fault systems (Fig. 2D); and (3) sites RR4 and RR8 are close to the unconformity with Cretaceous beds and site RR2 is distant to the Cretaceous outcrop, therefore the two-step tilt correction is reliable for sites RR4 and RR8. For Lower Cretaceous directions, we consider the mean direction of component C1 obtained in Bosconia; we prefer to discard the direction of C1 in Mingueo sector due to high deformation of Cretaceous beds, and also because the information comes from only one site.

All components C2 in sector III (Fonseca) show evidence of clockwise rotations. The magnitude of clockwise rotation is 17 ± 12.8° using only sites RR4 and RR8 (Table 5) with respect to a stable point in the craton (Fig. 5); a greater magnitude (24.8 ± 38.3°) may be considered if the mean direction of sector III (Fonseca) is used; a smaller magnitude (9.1 ± 18.9°) result if

Table 5

Calculation of: (1) expected declination (Dm) and inclinations (Im) for a reference point in the stable craton (see Fig. 5 for location), virtual geomagnetic poles (VGP) from characteristic components C1 and C2 (Dm, Im) in the Santa Marta massif, (3) paleolatitudes, and (4) rotations of the Santa Marta massif relative to the reference point in the stable craton. VGP position for the South America craton recalculated using data from Castillo et al. (1991), Randall (1998) and Vizán et al. (2004).

	VGP			Direction			Paleolatitude			Rotation	
	Lat	Log	A95	Dm	Im	a95	Mean	South	North	Mean	Error
Aptian (112–121 Ma) direction (Dm Im) calculated in the Craton (4°N 72°W), using Southamerican paleopole	84.6	252.6	3.5	**356.8**	**16.4**	3.5	8.4	10.3	6.5		
Paleopole calculated for Aptian–Albian Component C1 in SMM (only Sector I, Bosconia, 10°N 73.7°W)	**79.6**	**48.5**	**9.8**	8.8	8.3	13.7	4.2	−1.7	10.5	12	14.3
Jurassic-Cretaceous (121–160 Ma) direction (Dm Im) calculated in the Craton (4°N 72°W), using Southamerican paleopole	84.2	220.7	5.2	**354.6**	**12.3**	5.2	6.2	9	3.6		
Middle Jurassic direction (Dm Im) calculated in the Craton (4°N 72°W), using Southamerican paleopole	−85.4	240.2	11.6	**3.4**	**1.8**	11.6	0.9	−4.9	6.8		
Component C2 in SMM (sites RR4 and RR8 of Sector III, Fonseca, 10.9°N 72.9°W)	**−61.3**	**241.3**	**3.8**	20.4	−18.2	5.1	−9.3	−12.2	−6.6	17	12.8

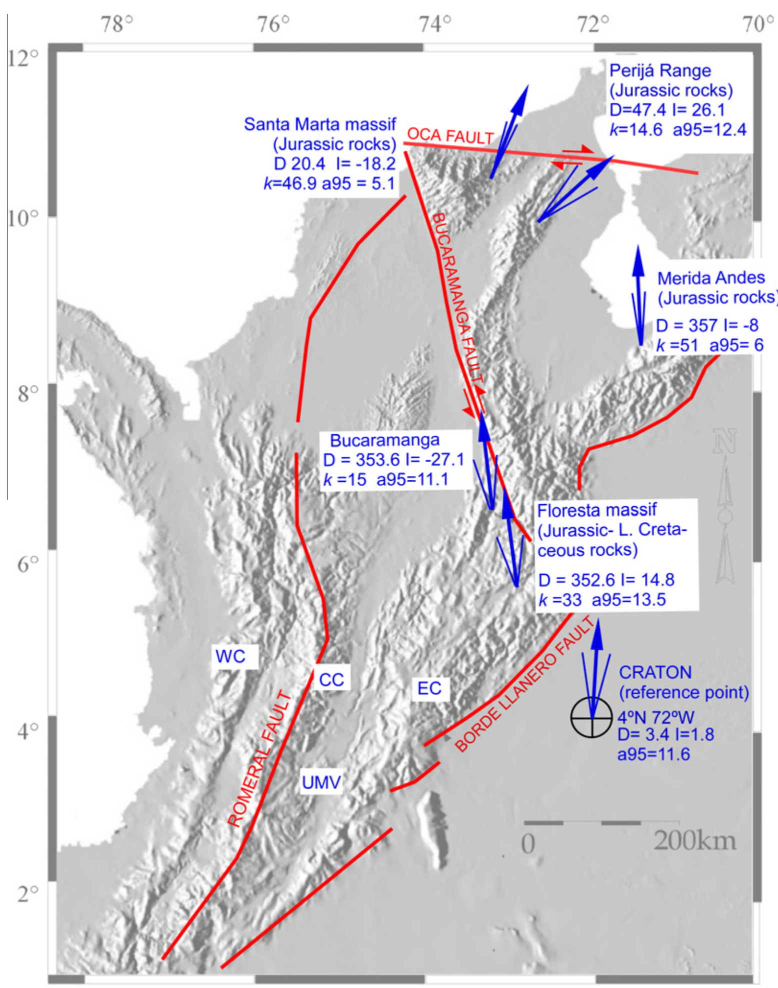

Fig. 5. Comparison of Jurassic and Cretaceous characteristic paleomagnetic declination reported for the Santa Marta massif (component C2), Perija Range (Gose et al., 2003), Merida Andes (mean of Jurassic La Quinta Fm.; Castillo et al., 1991), Bucaramanga (Jordan Fm.), Floresta massif (Giron-Tibasosa units) and an arbitrary point in the craton (Bayona et al., 2006b) (see Table 1 for other statistical parameters). Clockwise rotation of the Santa Marta massif and Perija Range, with respect to the craton, is 17 ± 12.8° and 50 ± 12°, respectively.

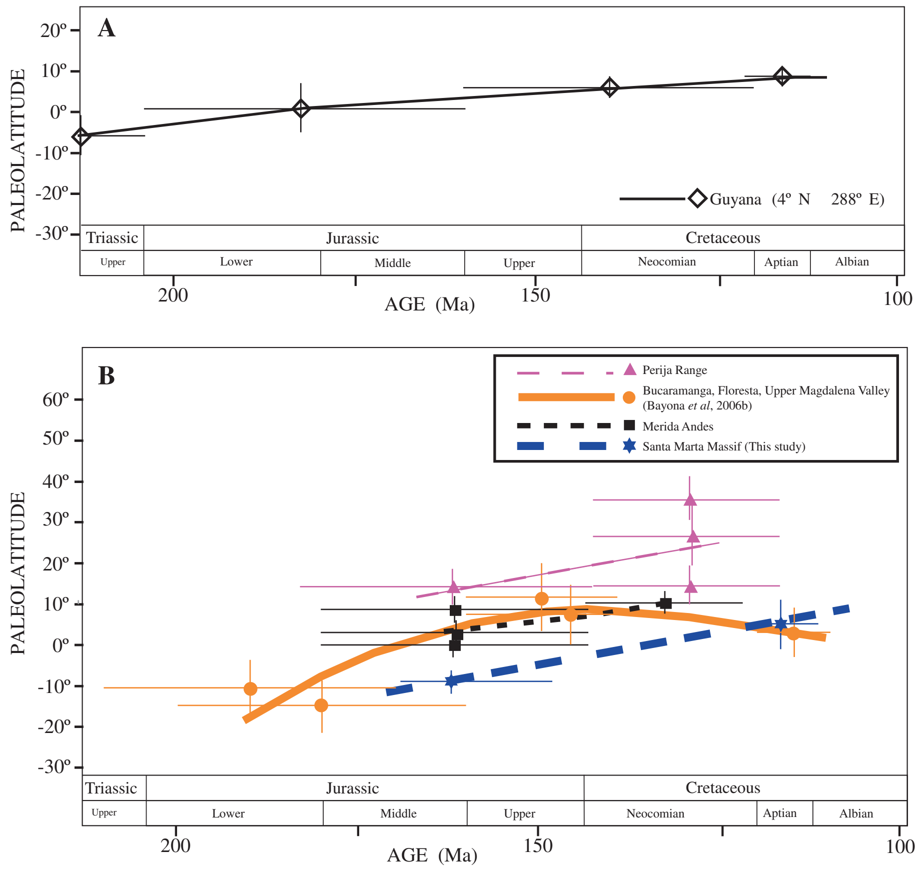

Fig. 6. Paleolatitude data calculated using paleomagnetic data from Upper Triassic to Lower Cretaceous rocks in (A) the stable craton (paleopole recalculated using data from Castillo et al. (1991), Randall (1998), and Vizán et al. (2004)) and (B) The Santa Marta massif and other ranges in the northern Andes. Note the contrasting difference in paleolatitudinal displacement of the craton with respect to the Santa Marta massif in Early to Middle Jurassic time (see Table 1 for data).

the mean direction of component C2 is from sectors I, II and III. Similar sense, but with higher magnitude of rotations (50 ± 12°), has been documented for the Perija Range (Gose et al., 2003). Clockwise rotation is also inferred for C1 component in Sector I (Bosconia, 12° ± 14.3°)(Table 5), but the magnitude may be affected by local structural complexity. Montes et al. (this volume) discuss the implications of clockwise rotation for Neogene extensional tectonism of the Lower Magdalena basin along the western (trailing) border of the Santa Marta massif, and Neogene thrusting along the southeastern (leading) border to the Santa Marta massif.

Comprehensive analysis of our results together with paleomagnetic data from Jurassic to Lower Cretaceous rocks exposed in the Perijá Range, Mérida Andes, Eastern Cordillera, southern Magdalena Valley and stable areas of South America shows northward translation of terranes west of the Borde Llanero Faults with respect to the craton (data from Bayona et al., 2006b; Fig. 6). In the Early Jurassic, mean-paleolatitude values for terranes west of the Borde Llanero and Bucaramanga faults varies from −14.4° (Bucaramanga area), −12.7° (Santa Marta massif) to −10.5° (Upper Magdalena Valley), but these values change significantly in the Late Jurassic–Early Cretaceous to +4.2° (Santa Marta massif), +7.5° (Floresta Massif), +11.3° (BA) and +3.1° (Upper Magdalena Valley) (see Table 3; Fig. 6 shows error bars for paleolatitudinal and age determinations). Northward translation of mean-paleolatitudinal values of a reference point in the craton (4°N, 72°W, see position in Figs. 1A and 5) from Early Jurassic to Early Cretaceous was only from +0.9° to +6.2° (Table 3; Fig. 6). Northern (positive) paleolatitudes have been determined in Jurassic rocks exposed in the Merida Andes (Castillo et al., 1991) and Perija Range (Gose et al., 2003).

7.4. Paleogeographic reconstructions for the evolution of the northwestern margin of South America

The early Mesozoic conceptual tectonic evolution presented here illustrates along-margin northward translation of terranes with respect a reference point in the craton (Fig. 7). This model is supported by paleomagnetic data, and considers both geochemical and stratigraphic data of lower Mesozoic rocks presented in Bayona et al. (2006b). The model is based on the suggestion of northward displacement of accreted terranes during the Late Jurassic in a greater magnitude than the northward displacement of a reference point in the South America craton (Fig. 6). In Late Triassic to Early Jurassic times, the South American craton was subject of considerable paleolatitudinal movements (Iglesia et al., 2006); we do not have data from rocks of those ages in accreted terranes to make a comparison in the difference of displacement between accreted terranes and the stable craton.

The restored position of translated continental-cored terranes, now disrupted at different latitudes in the Colombian Andes (Fig. 1A), may help to define the extension of marine basins, fossil associations and presence of paleosol profiles. Ordovician graptolites reported in the Upper Magdalena Valley have affinities with Graptolites reported in northern Argentina (Moreno et al., 2008), and Geyer (1969) noted a similar upper Triassic–Lower Jurassic ammonites association in San Lucas Range and northern Peru. The similarity between the early Mesozoic stratigraphy and tectonic setting of the Southern Magdalena Valley, San Lucas range and Santa Marta massif with the upper Permian – lower Jurassic volcanics, red beds, and marine limestones, shales and sandstones

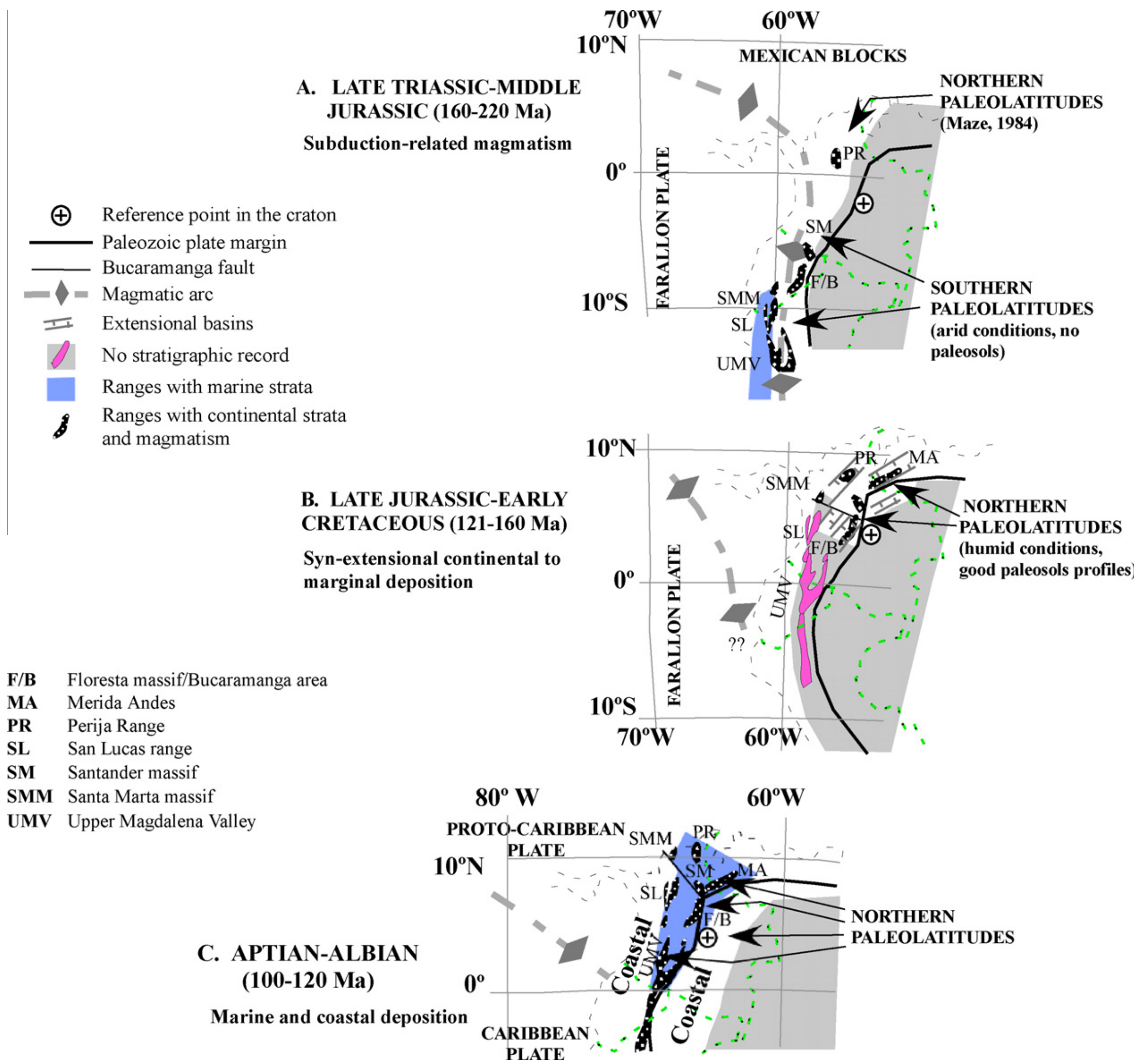

Fig. 7. Conceptual model of along-strike migration of accreted terranes in an oblique subduction margin, modified from Bayona et al. (2006b). See Fig. 1A for present geographic distribution of massifs and other structural blocks in northern South America. (A) Calc-alkaline plutonic and volcanic rocks are aligned along a linear subduction-related magmatic arc. (B) Translations changed to a dominantly east–west direction, as suggested by Castillo et al. (1991). Extensional tectonism affected areas close to the Bucaramanga fault (FM, SM, PR, MA), which acted as a transfer fault. (C) For Aptian time, the terrains are juxtaposed to the stable craton.

in Eastern Cordillera of Peru and Bolivia indicate that the areas were adjacent in early Mesozoic times (Sempere et al., 2002; Sarmiento-Rojas et al., 2006). Marine strata of upper Triassic–Lower Jurassic Indios Formation in the Santa Marta massif (Trumpy, 1943 in Etayo-Serna et al., 1983), the Morrocoyal Formation in San Lucas Range (Geyer, 1969) and those from Southern Magdalena Valley (Mojica and Prinz-Grimm, 2000), may have accumulated in the same extensional basin of marine strata now exposed in Ecuador (Santiago Fm., Geyer, 1974 in Mojica et al., 1996) and northern Peru (Jaillard et al., 1990; Sempere et al., 2002) (Fig. 7A). Paleomagnetic data from Permian and Triassic rocks in northern Peru indicate no significant paleolatitudinal transport and rotations with respect the stable craton (Gilder et al., 2003).

The change from red, laminated mudstones interbedded with bioturbated to massive sandstones accumulated in marginal lacustrine to fluvial settings of the of the Middle Jurassic Jordan Formation (Cediel, 1968) to mottled massive mudstones with concoidal fracture in the Jurassic–Lower Cretaceous Giron Formation (Ayala-Calvo et al., 2005) may suggest that paleosol development in continental successions is the result of a change from arid to more humid conditions. This change in climatic conditions may be explained by the hypothesis of northward translations of terranes.

The distribution of Grenvillian crust in the northern Andes suggest that Grenvillian belts of the Colombian Andes will fit a position closed to northern Peru and Southern Ecuador during the Jurassic, leaving room for several Mexican pre-Mesozoic terranes that overlap the northwestern margin of Colombian and Venezuela between the Early Pemian and the Early Jurassic (Pindell and Barret, 1990; Dickinson and Lawton, 2001; Cardona et al., 2009).

In summary, the tectonic model illustrated in Fig. 7 shows two major tectonic events affecting the northwestern margin of South America. The first tectonic scenario occurred during the Late Triassic and Early Jurassic and is related to an oblique subduction margin (Fig. 7A). Calc-alkaline magmas intruded along a magmatic arc striking parallel to the subduction zone (Aspden et al., 1987). This magmatic arc includes from north to south: Santa Marta massif, Santander massif, Floresta massif, San Lucas range and Upper Magdalena Valley, and due to the obliquity of its associated subduction, several arc, fore-arc and back-arc elements were displaced along the margin, as similar to the so called transcurrent or fore-arc terranes (Avé Lallement and Oldow, 1988; Gibbons, 1994). In Middle–Late Jurassic to Early Cretaceous (Fig. 7B), northward translations of terranes increase, westward retreat of the subduction zone and opening of the proto-Caribbean sea favored intracontinental extensional and/or transtensional deformation with development of basins filled by syn-extensional siliciclastic and volcaniclastic continental deposits in Merida Andes and Perija range, as well as in basins close to the Bucaramanga fault. For Early Cretaceous, diachronous marine transgression inundated the latter basins and reached its maximum extension in mid to Late Cretaceous time (Etayo-Serna et al., 1976) (Fig. 7C).

Additional paleomagnetic, structural and geochronological work is needed, including the adjacent San Lucas Range, in order to establish a more confident paleolatitudinal position for each accreted terranes.

8. Conclusions

Low to moderate temperature/coercivity magnetic components and moderate to high-temperature/coercivity characteristic magnetic components were successfully uncovered in Mesozoic rocks exposed in the Santa Marta massif (Fig. 1A).

The directions of those components are: a component whose direction is parallel to the present day Field (Component A: $D = 352$, $I = 25.6$, $k = 57.35$, a95 = 5.3, $N = 12$), a second component uncovered in Lower Cretaceous and Jurassic rocks with reset K–Ar ages (Component C1: $D = 8.8$, $I = 8.3$, $k = 24.71$, a95 = 13.7, $N = 6$), and a third component only uncovered in Jurassic volcaniclastic rocks (Component C2: $D = 12.5$, $I = -12$, $k = 13.38$, a95 = 14.6, $N = 8$). The tilt test is not statistically significant due to similar dip directions of Mesozoic strata, but the following arguments support a Middle–Late Jurassic age as the time of magnetization, close to the time of deposition: (1) direction is different than that of components A and C1; (2) high stability of components; (3) better cluster of moderate negative inclinations after the two steps of tilt corrections; and (4) K–Ar ages are in Middle–Late Jurassic range. Similar directions have been reported in other Middle Jurassic rocks south of Bucaramanga (Jordan Formation) and southern Magdalena Valley (Saldaña Formation) (Fig. 1B; Bayona et al., 2006a,b).

Characteristic component C2 was isolated in eight sites, However, only two sites have reliable age and structural data. These two sites are in the Fonseca sector, the area with the least structural complexity and good structural control; overlying Cretaceous rocks are very close to having a reliable unconformity test. In addition, a K–Ar age of 156.6 ± 8.9 Ma was obtained in one of those sites. The mean direction calculated from these two sites is $D = 20.4$, $I = -18.2$, $k = 46.9$, a95 = 5.1, $n = 18$ specimens from two sites, and we use this direction to estimate rotation and terrane translation. The magnitude of clockwise rotation is $17 \pm 12.8^\circ$ with respect to a stable point in the craton. A similar sense of rotation has been proposed for the Perija Range, but with a magnitude of $50 \pm 12^\circ$ (Gose et al., 2003). The Santa Marta massif moved northward from -9.3° at Middle Jurassic time, to $+4.2^\circ$ in Early Cretaceous time, and then to its present latitude $+10^\circ$. Similar northward movement in other terranes south of the Bucaramanga fault, restored configurations of Late Triassic–Early Jurassic marine strata, and differences of paleosol development favour the hypothesis of along-strike paleolatitudinal migration of terranes (Bayona et al., 2006b).

The preliminary paleomagnetic results and obtained K–Ar ages suggest the need for a more detailed paleomagnetic study in the Fonseca sector. This study should include magnetic mineral analysis together with a stratigraphy and U–Pb geochronology of the Jurassic volcaniclastic succession to better quantify the magnitudes of rotations and translations of the Santa Marta massif. Paleo-magnetic studies in the Bosconia sector may clarify local rotations associated with reverse and strike–slip fault systems.

Acknowledgements

This research was funded by Ingeominas, Instituto Colombiano del Petroleo and Invemar. We acknowledge Ricardo Trindade and Danielle Brant (University of Sao Paulo), and James Channell and Kainian Huang (University of Florida) for assistance and discussion of paleomagnetic data during our work in the Paleomagnetic Laboratories. The field geologist group of Geosearch Ltda contributed to the location of sites during the 2006–2007 field seasons. Johana Casas helped for access to the construction and tunnel of the Rancheria Dam, and Ivan Gutierrez helped in the collection of the samples. We thanks to Georgina Guzman (Invemar) for allowing us the publication of segments of the geologic map of the Sierra Nevada de Santa Marta (Invemar–Ingeominas–Ecopetrol – ICP-Geosearch Ltda, 2007). Comments and suggestions from Roberto Moliza Garza, Victoria Mejia and an anonymous reviewer contributed to improve the presentation of data and content of the manuscript.

References

Aspden, J.A., McCourt, W.J., Brook, M., 1987. Geometrical control of subduction-related magmatism: the Mesozoic and Cenozoic plutonic history of western Colombia. Journal of the Geological Society 144, 893–905.

Avé Lallement, H., Oldow, J., 1988. Early Mesozoic migration of Cordilleran transpressional terranes. Tectonics 7, 1057–1075.

Ayala-Calvo, R.C., Veloza, G.E., Bayona, G., Gómez-Casallas, M., Rapalini, A.E., Costanzo-Álvarez, V., Aldana, M., 2005. Paleomagnetismo y mineralogía magnética en las unidades del Mesozoico de Bucaramanga y Macizo de Floresta. Geología Colombiana 30, 49–66.

Bayona, G., Jaramillo, C., Reyes-Harker, A., 2006a. Resultados Paleomagnéticos en unidades del Paleógeno de Colombia y Oeste de Venezuela y posibles usos para caracterización de contactos. Geología Colombiana 31, 57–72.

Bayona, G., Rapalini, A.E., Costanzo-Álvarez, V., 2006b. Paleomagnetism in mesozoic rocks of the northern Andes and its implications in mesozoic tectonics of northwestern Southamerica. Earth Planets and Space 58, 1255–1272.

Bayona, G., Jaramillo, C., Rueda, M., Reyes-Harker, A., Torres, V., 2007. Paleocene–middle Miocene flexural-margin migration of the nonmarine Llanos foreland basin of Colombia. CT&F Ciencia, Tecnología y Futuro 3 (3), 141–160.

Bellizzia, G.A., Pimentel, M.N., Bajo, O.R., 1976. Mapa Geológico Estructural de Venezuela. Plancha Nc-18-I Manchiques, Foninves. Caracas, Venezuela.

Caceres, H., Camacho, R., Reyes, J., 1980. The Geology of the Rancheria Basin. In: Geotec (Ed.), Geological Field-Trips, Colombia 1980–1989. Asociación Colombiana de Geólogos y Geofísicos del Petróleo, Bogotá, pp. 1–31.

Cardona, A., Duque, J., Ruiz, J., Valencia, V., Bayona, G., Jaramillo, C., Ojeda, G., Orozco, M., 2008. Geochronology and tectonic implications of granitoids rocks from the northwestern Sierra Nevada de Santa Marta and surrounding basins, northeastern Colombia. In: Late Cretaceous to Paleogene Convergence, Accretion and Subduction Interactions between the Caribbean and South American Plate, 18th Geological Caribbean Conference, Dominican Republic, p. 12.

Cardona, A., Chew, D., Valencia, V., Bayona, G., Miskovic, A., Ibañez, M., 2010. Grenvillian remnants in the northern Andes: Rodinia and Phanerozoic paleogeographic perspectives. Journal of South American Earth Sciences (Special Issue: Grenville) 29, 92–104.

Cardona, A., Valencia, V., Bayona, G., Jaramillo, C., Ojeda, G., Ruiz, J., 2009. U/Pb LAM-ICP-MS zircon geochronology and geochemistry from a post-collisional biotite granite of the Baja Guajira basin, Colombia; implications for Late Cretaceous and Neogene Caribbean-South America tectonics. The Journal of Geology 117, 685–692.

Cardona-Molina, A., Cordani, U., MacDonald, W.D., 2006. Tectonic correlations of pre-Mesozoic crust from the northern termination of the Colombian Andes, Caribbean region. Journal of South American Earth Sciences 21, 337–354.

Castillo, J., Gose, W.A., Perarnau, A., 1991. Paleomagnetic results from Mesozoic strata in the Mérida Andes, Venezuela. Journal of Geophysical Research 96, 6011–6022.

Cediel, F., 1968. El Grupo Girón: una molasa Mesozoica de la Cordillera Oriental. Servicio Geológico Nacional. Boletin Geológico XVI, pp. 5–96.

Cediel, F., Shaw, R., Cáceres, C., 2003. Tectonic assembly of the Northern Andean block. In: Bartolini, C., Buffler, R., Blickwede, J. (Eds.), The Circum-Gulf of Mexico and the Caribbean: Hydrocarbon Habitats, Basin Formation and Plate Tectonics, 79. American Association of Petroleum Geologists Memoir, pp. 815–848.

Clavijo, J., Mantilla, L., Pinto, J., Bernal, L., Pérez, A., 2008. Evolución Geológica de la Serranía de San Lucas, Norte del Valle Medio del Magdalena y Noroeste de la Cordillera Oriental. Boletín de Geología de la UIS 30, 45–62.

Cooper, M.A., Addison, F.T., Alvarez, R., Coral, M., Graham, R.H., Hayward, A.B., Howe, S., Martínez, J., Naar, J., Peñas, R., Pulham, A.J., Taborda, A., 1995. Basin development and tectonic history of the Llanos basin, Eastern Cordillera, and Middle Magdalena Valley, Colombia. American Association of Petroleum Geologists Bulletin 79, 1421–1443.

Cordani, U.G., 1970. Idade do Vulcanismo no Océano Atlántico Sul. Boletim do Institute Astronómico e Geofísico, Universidade de Sao Paulo, vol. 1, pp. 9–75.

Cordani, U.G., Ulbrich, M.N.C., Onoe, A.T., Vinasco, C.J., 2004. Novas determinacoes de idade pelos métodos K–Ar e Ar/Ar para o Arquipélago de Fernando de Noronha. Revista da Facultade de Ciencias, Universidade Eduardo Mondlade 1, 167–178.

Cordani, U., Cardona, A., Jiménez, D., Liu, D., Nutman, A., 2005. Geochronology of Proterozoic basement inliers from the Colombian Andes: Tectonic history of Remnants from a fragmented Grenville belt. In: Vaughan, A.P.M., Leat, P.T., Pankhurst, R.J. (Eds.), Terrane Processes at the Margins of Gondwana, vol. 246. Geological Society of London Special Publication, pp. 329–346.

Dasch, L.E., 1982. U–Pb Geochronology of the Sierra de Perijá. Doctoral thesis. Case Western Reserve University, 163 p.

Demarest, H., 1983. Error analysis for determination of tectonic rotation from paleomagnetic data. Journal of Geophysical Research 88, 4321–4328.

Dickinson, W.R., Lawton, T.F., 2001. Carboniferous to Cretaceous assembly and fragmentation of Mexico. Geological Society of America Bulletin 113, 1142–1160.

Dueñas, H., 2002. Paleozoic Palynological Assemblages from the Llanos Orientales Basin, Colombia. In: 2da Convención Técnica de la A.C.G.G.P. (Eds.), Geología y Petróleo en Colombia – Fronteras de Exploración, Colombia. CD Memoirs.

Estrada, J., 1995. Paleomagnetism and accretion events in the northern Andes. Ph.D. Dissertation thesis. New York State University, 172 p.

Etayo-Serna, F., Renzoni, G., Barrero, D., 1976. Contornos sucesivos del mar Cretácico en Colombia. In: Primer Congreso Colombiano de Geología, Memorias, Bogotá, pp. 217–252.

Etayo-Serna, F., Barrero, D., Lozano, H., et al., 1983. Mapa de terrenos geológicos de Colombia, Ingeominas, Bogotá, 235 p.

Faure, G., 1986. Principles of Isotope Geology. John Wiley & Sons. 589 p.

Fisher, R.A., 1953. Dispersion on a sphere. Proceedings of the Royal Society of London, Series A217, 295–305.

Forero, A., 1990. The basement of the Eastern Cordillera, Colombia: an allochthonous terrane in northwestern South America. Journal of South American Earth Sciences 3, 141–151.

Geyer, O., 1969. La fauna de amonitas del perfil típico de la Formación Morrocoyal. In: Primer Congreso Colombiano de Geología, Memorias, Bogotá, pp. 111–134.

Gibbons, W., 1994. Suspect terranes. In: Hackock, P. (Ed.), Continental deformation. Pergamon Press, pp. 305–319.

Gilder, S., Rousse, S., Farber, D., McNulty, B., Sempere, T., Torres, V., Palacios, O., 2003. Post-Middle Oligocene origin of paleomagnetic rotations in Upper Permian to Lower Jurassic rocks from northern and southern Peru. Earth and Planetary Science Letters 210, 233–248.

González de Juana, C., Iturralde, J., Picard, J., 1980. Geología de Venezuela y de sus Cuencas Petrolíferas. Ediciones Foninves. Caracas, Venezuela.

Gose, W.A., Perarnau, A., Castillo, J., 2003. Paleomagnetic results from the Perijá Mountains, Venezuela: an example of vertical axis rotation. In: Bartolini, C., Buffler, R., Blickwede, J. (Eds.), The Circum-Gulf of Mexico and the Caribbean, Hydrocarbon Habitats, Basin Formation and Plate Tectonics, 79. AAPG Memoir, pp. 969–975.

Iglesia, M.P., Ricarddi, A., Singer, S., 2006. Paleomagnetic study of Lower Cretaceous marine strata from the Neuquen basin, Argentina: a new Jurassic apparent polar wander path for South America. Earth and Planetary Science Letters 252, 379–397.

Invemar–Ingeominas–Ecopetrol – ICP-Geosearch Ltda, 2007. Geologic map of the Sierra Nevada de Santa Marta, scale 1:200.000.

Jaillard, E.P., Solar, P., Carlier, G., Mourier, T., 1990. Geodynamic evolution of the northern and central Andes during early to middle Mesozoic times: a Tethyan model. Journal of the Geological Society of London 147, 1009–1022.

Jiménez, D., Juliani, C., Cordani, U., 2006. P–T–t conditions of high-grade metamorphic rocks of the Garzón Massif, Andean basement, SE Colombia. Journal of South American Earth Sciences.

Kerr, A., Tarney, J., 2005. Tectonic evolution of the Caribbean and northwestern South America: the case for accretion of two Late Cretaceous oceanic plateaus. Geology 33, 269–272. doi:10.1130/G21109.1.

Kirschvink, J., 1980. The least-squares line plane and the analysis of palaeomagnetic data. Geophysical Journal of the Royal Astronomical Society 62, 699–718.

MacDonald, W.D., Opdyke, N.D., 1984. Preliminary paleomagnetic results from Jurassic rocks of the Santa Marta Massif, Colombia. In: Bonini, W.E., Hargraves, R.B., Shagam, R. (Eds.), The Caribbean–South American plate boundary and regional tectonics, vol. 162. Geological Society of America Memoir, pp. 295–298.

MacDonald, D., Doolan, B., Cordani, U., 1971. Cretaceous-early Tertiary metamorphic age values from the South Caribbean. Geological Society of America Bulletin 82 (5), 1381–1388.

Maze, W., Hargraves, R.B., 1984. Paleomagnetic results from the Jurassic La Quinta Formation in the Perijá range, Venezuela, and their tectonic significance. The Caribbean–South American Plate Boundary and Regional Tectonics, vol. 162. Geological Society of America, Memoir, pp. 287–293.

Mcdougall, I., Harrison, T.M., 1999. Geochronology and thermochronology by the Ar/Ar method. Oxford University Press. 269 p.

McElhinny, M.W., 1964. Statistical significance of the fold test in paleomagnetism. Geophysical Journal of the Royal Astronomical Society 8, 338–340.

McFadden, P.L., Reid, A.B., 1982. Analysis of paleomagnetic inclination data. Geophysical Journal of the Royal Astronomical Society 69, 307–319.

Miller, J.B., 1962. Tectonic Trends in Sierra De Perija and Adjacent Parts of Venezuela and Colombia. AAPG Bulletin 46, 1565–1595.

Mojica, J., Prinz-Grimm, P., 2000. Las faunas de Amonitas del Triásico Tardío en el miembro Chicalá (parte baja de la Formación Saldaña) en Payandé, Tolima, Colombia. Geología Colombiana 25, 13–23.

Mojica, J., Kammer, A., Ujueta, G., 1996. El Jurásico del sector noroccidental de Suramérica y guía de la excursión al Valle Superior del Magdalena (Nov. 1–4/95), Regiones de Payandé y Prado, Departamento del Tolima, Colombia. Geología Colombiana 21, 3–40.

Montes, C., Hatcher Jr., D., Restrepo-Pace, P., 2005. Tectonic reconstruction of the northern Andean blocks: Oblique convergence and rotations derived from the kinematics of the Piedras-Girardot area, Colombia. Tectonophysics 399 (1–4), 221–250.

Montes, C., Guzman, G., Bayona, G., Cardona, A., Valencia, V., Jaramillo, C., this volume. Clockwise rotation of the santa marta massif and simultaneous paleogene to neogene deformation of the Plato-San Jorge and Cesar-Rancheria basins. Journal of South American Earth Sciences.

Moreno, M., Gómez, A., Castillo, H., 2008. Graptolitos del Ordovícico y Geología de los Afloramientos del Río Venado (Norte del Departamento del Huila). Universidad Industrial de Santander, Bucaramanga. Boletín de Geología 30 (1), 9–19.

Ostos, M., Yoris, F., Avé Lallemant, H.G., 2005. Overview of the southeast Caribbean–South American plate boundary zone. In: Avé Lallemant, H.G., Sisson, V.B. (Eds.), Caribbean–South American plate interactions, Venezuela, vol. 394. Geological Society of America Special Paper, pp. 53–89.

PDVSA-INTEVEP, 2005. Léxico Estratigráfico de Venezuela. In: Comité Interfilial de Estratigrafía y Nomenclatura (Eds.), <www.pdvsa.com/lexico/lexicoh.htm>.

Pindell, J.L., Barret, S.F., 1990. Geological evolution of the Caribbean region: a plate tectonic perspective. In: Dengo, G., Case, J. (Eds.), The Caribbean region. v. H. The Geology of North America. Geological Society of America, pp. 405–432.

Priem, H., Kroonenberg, S., Boelrijk, N., Hebeda, E., 1982. Rb–Sr and K–Ar evidence for the presence of a 1.6 Ga basement underlying the 1.2 Ga Garzón-Santa Marta Granulite Belt in the Colombian Andes. Precambrian Research 42, 315–324.

Randall, D., 1998. A new Jurassic–Recent apparent polar wander path for South America and a review of central Andean tectonic models. Tectonophysics 299, 49–74.

Restrepo-Pace, P., 1992. Petrotectonic characterization of the central Andean terrane, Colombia. Journal of South American Earth Sciences 5 (1), 97–116.

Restrepo-Pace, P., Ruiz, J., Gehrels, G., Cosca, M., 1997. Geochronology and Nd isotopic data of Grenville-age rocks in the Colombian Andes: new constraints for Late Proterozoic–Early Paleozoic paleocontinental reconstructions of the Americas. Earth and Planetary Science Letters 150, 427–441.

Sarmiento-Rojas, L.F., Van Wess, J.D., Cloetingh, S., 2006. Mesozoic transtensional basin history of the Eastern Cordillera, Colombian Andes: inferences from tectonic models. Journal of South American Earth Sciences 21, 383–411.

Sempere, T., Carlier, G., Soler, P., Fornari, M., Carlotto, V., Jacay, J., Néraudeau, D., Cárdenas, J., Rosas, S., Jímenez, N., 2002. Late Permian–Middle Jurassic lithospheric thinning in Peru and Bolivia, and its bearing on Andean-age tectonics. Tectonophysics 345, 153–181.

Steiger, R.H., Jager, E., 1977. Subcommission on geochronology: convention on the use of the decay constants in geo- and cosmochronology. Earth and Planetary Science Letters 36, 359–362.

Tschanz, C., Jimeno, A., Vesga, C., 1969. Geology of the Sierra Nevada de Santa Marta area, Colombia. Ingeominas.

Tschanz, C., Marvin, R., Cruz, J., Mennert, H., Cebula, E., 1974. Geologic evolution of the Sierra Nevada de Santa Marta. Geological Society of America Bulletin 85, 269–276.

Vásquez, M., Bayona, G., Romer, R. L., 2006. Geochemistry of Jurassic volcanic Rocks of the Northern Andes: Insights for the Mesozoic Evolution of the Northwestern corner of the Southamerica plate. In: 2006 Backbone of the Americas, Mendoza, Argentina.

Vizán, H., Ixer, R., Turner, P., Cortés, J.M., Cladera, G., 2004. Paleomagnetism of Upper Triassic rocks in the Los Colorados hill section, Mendoza province, Argentina. Journal of South American Earth Sciences 18, 41–59.

Ward, D., Goldsmith, R., Cruz, J., Restrepo, H., 1973. Geología de los Cuadrángulos H-12, Bucaramanga y H-13, Pamplona, Departamento de Santander. Ingeominas, Boletín Geológico 21 (1–3), 132.

Zijderveld, J.D.A., 1967. A.C. demagnetization of rocks: analysis of results. In: Collison, D.W., Creer, K.M., Runcorn, S.K. (Eds.), Methods of Paleomagnetism. Elsevier Science, pp. 254–286.